Scaling and a Fokker-Planck model for fluctuations in geomagnetic indices and comparison with solar wind ϵ as seen by Wind and ACE

B. Hnat, S. C. Chapman, and G. Rowlands
Space and Astrophysics Group, University of Warwick, Warwick, UK

Received 5 October 2004; revised 23 March 2005; accepted 23 May 2005; published 24 August 2005.

[1] The evolution of magnetospheric indices on temporal scales shorter than that of substorms is characterized by bursty, intermittent events that may arise from turbulence intrinsic to the magnetosphere or that may reflect solar wind-magnetosphere coupling. This leads to a generic problem of distinguishing between the features of the system and those of the driver. We quantify scaling properties of short-term (up to few hours) fluctuations in the geomagnetic indices *AL* and *AU* during solar minimum and maximum, along with the parameter ϵ that is a measure of the solar wind driver. We find that self-similar statistics provide a good approximation for the observed scaling properties of fluctuations in the geomagnetic indices, regardless of the solar activity level, and in the ϵ parameter at solar maximum. This self-similarity persists for fluctuations on timescales at least up to about 1–2 hours. The scaling exponent of *AU* index fluctuations show dependence on the solar cycle, and the trend follows that found in the scaling of fluctuations in ϵ. The values of their corresponding scaling exponents, however, are always distinct. Fluctuations in the *AL* index are insensitive to the solar cycle, as well as being distinct from those in the ϵ parameter. This approximate self-similar scaling leads to a Fokker-Planck model which, we show, captures the probability density function of fluctuations and provides a stochastic dynamical equation (Langevin equation) for time series of the geomagnetic indices.

Citation: Hnat, B., S. C. Chapman, and G. Rowlands (2005), Scaling and a Fokker-Planck model for fluctuations in geomagnetic indices and comparison with solar wind ϵ as seen by Wind and ACE, *J. Geophys. Res.*, *110*, A08206, doi:10.1029/2004JA010824.

1. Introduction

[2] The Earth's magnetosphere can be considered as nonlinear, dissipative system which is driven by the time varying solar wind. Accumulated energy is ultimately dissipated, at least in part, through a system of currents generated in the auroral zones of the ionosphere. These currents produce small changes in the terrestrial magnetic field which can be used to monitor magnetospheric activity. The complex behavior of the magnetosphere, as suggested by many observations [see, e.g., *Horton et al.*, 1999; *Lewis*, 1991; *Sitnov et al.*, 2000; *Takalo et al.*, 2000; *Vassiliadis et al.*, 2000; *Vörös et al.*, 2002], could then be attributed either to intrinsic magnetospheric processes, the complex nature of its coupling with the solar wind and the ionosphere or both.

[3] Recent observations suggest that the multiscale nature of this coupling is a fundamental aspect of magnetospheric dynamics [see, e.g., *Chang*, 1992; *Chapman and Watkins*, 2001; *Klimas et al.*, 1996; *Ukhorskiy et al.*, 2003; *Vassiliadis et al.*, 2003; *Weigel et al.*, 2003]. Evidence is provided by a variety of observations which exhibit statistical properties previously identified as hallmarks of multiscale systems. For example, bursty transport events have been reported in the magnetotail [*Angelopoulos et al.*, 1992] and their auroral signatures suggest self-similar statistics [*Lui et al.*, 2000; *Uritsky et al.*, 2001, 2002b, 2003; *Kozelov et al.*, 2004]. The fluctuations in the ground based measurements of the magnetic field are non-Gaussian and also exhibit scaling [*Consolini et al.*, 1996; *Kovács et al.*, 2001; *Vörös et al.*, 1998]. In the context of time series analysis, geomagnetic indices are of particular interest as they provide a global measure of magnetospheric output and are evenly sampled over a long time interval. These indices also show non-Gaussian statistics of fluctuations and anomalous scaling over the short timescales of up to few hours [*Consolini and De Michelis*, 1998; *Takalo et al.*, 1993; *Hnat et al.*, 2003a; *Stepanova et al.*, 2003; *Tsurutani et al.*, 1990]. The extent to which observed statistical features of the geomagnetic indices arise directly from those of the solar wind driver or the auroral currents is of fundamental interest. This is an example of the generic problem of distinguishing between features intrinsic to a driven system and those in the driver, when both show scaling. Some recent studies has focused on direct comparison of scaling properties of the driver with these found in the geomagnetic

0148-0227/05/2004JA010824$09.00

indices [*Freeman et al.*, 2000; *Uritsky et al.*, 2001; *Hnat et al.*, 2003a] to establish whether, to the lowest order, they are directly related.

[4] The difficulty with interpreting these observations arises from the fact that statistical features described above can be recovered from many existing models. Self-organized criticality (SOC) and turbulence have both been extensively used [*Angelopoulos et al.*, 1999; *Consolini and De Michelis*, 1998; *Klimas et al.*, 2004a, 2004b; *Kozelov and Kozelova*, 2003; *Uritsky and Pudovkin*, 1998; *Uritsky et al.*, 2002a] in the past. Practically, one needs to obtain experimental constrains with which different models with similar characteristics can be tested. In this paper we present one possible approach to characterizing the time series in the context of scaling that does not rely on a specific model of multiscale systems [*Sornette*, 2000; *Hnat et al.*, 2003a]. The aim is to obtain statistical scaling properties directly from the data.

[5] Here, we will examine the statistical properties of Akasofu's ϵ [*Perreault and Akasofu*, 1978] parameter, which represents the energy input from the solar wind into the magnetosphere, and that of magnetospheric response as seen by the geomagnetic indices. Previously, scaling has been quantified over a 10 year data set for the indices and a comparison between $\delta\epsilon$ and the indices included, but was not restricted to, the solar minimum (1984–1987) [*Hnat et al.*, 2003a]. Here, we will perform this comparison over intervals of solar minimum and maximum separately. The statistical description of the experimental data will be extended to 10 standard deviations of the fluctuations.

[6] To facilitate the comparison of all considered quantities we will first explore to what extend their fluctuations exhibit approximate self-similar scaling for temporal scales of 1–2 hours. The quality of this self-similar approximation combined with values of the scaling exponents obtained at the solar minimum and maximum can be used to characterize each quantity. We will see that values of scaling exponents on these temporal scales for the geomagnetic indices are different from these found in the solar wind ϵ regardless of the phase of the solar cycle. Remarkably, the scaling exponent of the *AL* index is unchanged between solar minimum and maximum whereas the *AU* scaling exponent changes with the solar cycle. In this respect, the *AU* index seems to follow the trend found in the driver, ϵ i.e., the value of scaling exponent increases with increasing solar activity. We then construct a Fokker-Planck model for fluctuations in the geomagnetic indices and the ϵ at solar maximum as these exhibit the most satisfactory self-similar scaling. This allows us to obtain analytically a functional form of the fluctuation probability density function (PDF) which we can then check against the data. A stochastic dynamical model can then be formulated by considering the most general form of the Langevin equation and deriving functional forms of the coefficients that are consistent with the Fokker-Planck equation [see, e.g., *Hnat et al.*, 2003b].

2. Data and Methods

2.1. Data Sets

[7] To facilitate this analysis we used multiple data sets that spanned over different phases of the solar cycle. Two year intervals of data were selected centered on solar minimum and solar maximum. The solar wind data were obtained from WIND and ACE spacecraft observations. These were collected in the vicinity of the L1 point approximately 1 AU (Astronomical Units) from the Sun. The periods of coverage, final sampling frequencies and number of samples are given in the Table 1. The geomagnetic indices and the corresponding spacecraft data sets are not contiguous. The calibrated geomagnetic data set, from which intervals of interest has been selected, spans from January 1978 to December 1988 inclusive, while the spacecraft data are available starting from 1995 for WIND and 1998 for ACE. This available data coverage does not permit examination of successive solar cycles. We thus need to assume that the statistical properties of fluctuations are invariant from one solar cycle to the next. In the case of the spacecraft data, these include slow and fast solar wind streams.

[8] The solar wind velocity measurements, provided by the SWE instrument on board of WIND and ACE spacecraft, have varying temporal resolutions. In the case of WIND this resolution is in the range of 75–98 s while for the ACE spacecraft it changes between 60 and 120 s. The magnetometer data sets, on the other hand, have fixed temporal resolution of 46 s for WIND MFI instrument and 16 s in the case of the ACE magnetometer. The SWE data sets have been then resampled using linear interpolation to give uniform resolution of 92 s for WIND (twice the magnetometer resolution) and 64 s for the ACE spacecraft (four times magnetometer resolution). No other post processing, such as detrending or smoothing, was applied to data. The ϵ parameter is defined [*Perreault and Akasofu*, 1978] in SI units (Watts) as $\epsilon = v(B^2/\mu_0)\, l_0^2 \sin^4(\Theta/2)$, where $l_0 \approx 7R_E$ and $\Theta = \arctan(|B_y|/B_z)$, and was calculated from WIND and ACE spacecraft key parameter databases.

[9] All techniques discussed here are based on differencing of the original time series over a range of temporal scales τ. This method is often used in turbulence studies to compare the properties of fluctuations on different spatio-temporal scales [see, e.g., *Frisch*, 1995]. For a given time series $x(t)$ a set of differences $\delta x(t, \tau) = x(t + \tau) - x(t)$ will then capture fluctuations on temporal scale τ. Here, we will examine the statistical properties of the PDF of fluctuations $\delta x(t, \tau)$. The τ parameter will be given in power law form such as $\tau = \delta t_{AU}\,(1.2)^n$ s, where δt_{AU} is a sampling time of the *AU* time series (here, 1 min) and $n \geq 1$ is an integer. This choice of τ gives a uniform distance between points when plotted on the logarithmic scale while the small base of the power law (1.2) assures that the adequate number of temporal scales are explored. We stress that the differencing is performed only if both $x(t + \tau)$ and $x(t)$ exist and are separated by time interval τ.

2.2. Statistical Methods

[10] Generalized structure functions (GSF) S_m are widely used to characterize non-Gaussian processes [*Frisch*, 1995; *Hnat et al.*, 2003a]. These functions can be defined for fluctuations $\delta x(t, \tau)$ as $S_m(\tau) \equiv \langle |\delta x|^m \rangle$, where m can be any real number, not necessarily positive. If S_m exhibits scaling with respect to the time lag τ, for a sufficiently large range $\tau < \tau_{\max}$, we also have within that range $S_m \propto \tau^{\zeta(m)}$. In this case a log-log plot of S_m versus τ should reveal a straight line, extending up to $\tau_{\max}$, for each m and the gradients

Table 1. Data Sets Description

Quantity	Solar Cycle	dt, s	Dates	N, mln	Source
AL, *AU*	minimum	60	01/85 to 12/86	1.05	WDC STP
AL, *AU*	maximum	60	01/79 to 12/80	1.05	WDC STP
ϵ	minimum	92	08/95 to 07/97	0.63	WIND
ϵ	maximum	64	01/00 to 12/01	0.68	ACE

correspond to values of $\zeta(m)$. Generally, $\zeta(m)$ can be a nonlinear function of order m, however if $\zeta(m) = \alpha m$ (α constant) then the time series is self-similar (or more precisely, self-affine) with single scaling exponent α. This special case leads immediately to a Fokker-Planck description [*Hnat et al.*, 2003b]. The difficulty with computing GSF for higher orders, say, $m > 4$ arises from the slow convergence of this method and its sensitivity to large statistical errors in extremal events in the tails of the distribution. These effects can, as we shall see, lead to large errors in the estimation of $\zeta(m)$ (see also *Horbury and Balogh* [1997] for the discussion of error estimation for structure functions). One possible approach is to eliminate these extreme events from the fluctuation time series $\delta x(t, \tau)$ in a way that is consistent with the growth of the self-similar fluctuations' range on each temporal scale. This process is referred to as conditioning. Previously, a similar technique based on the wavelet filters has been used to separate the intermittent parts of the signal from the homogeneous noise in the *AE* index data [*Kovács et al.*, 2001]. We will condition our GSFs by imposing a threshold A on the fluctuation size [*Hnat et al.*, 2003a]. The threshold will be based on the standard deviation of the differenced time series for a given τ, $A(\tau) = 10\sigma(\tau)$. Under conditioning, the GSF can be expressed in term of the fluctuation PDF as:

$$\langle |\delta x|^m \rangle = \int_{-A}^{A} |\delta x|^m P(\delta x, \tau) d(\delta x). \quad (1)$$

This procedure is then consistent with scaling $\zeta(m) = m\alpha$ if it is present in the data, but for threshold A sufficiently large it does not enforce it on the data.

[11] The PDF rescaling technique is a generic and model-independent method of testing for statistical self-similarity in the data set. If the data is self-similar, then a single argument representation of the fluctuation PDF, $P_s(\delta x_s)$, can be found in the form:

$$P(\delta x, \tau) = \tau^{-\alpha} P_s(\delta x \tau^{-\alpha}), \quad (2)$$

where α is the rescaling exponent. This form of the PDF is also valid only up to a maximum temporal scale τ_{max}. Substituting the rescaled quantities P_s and $\delta x_s = \delta x \tau^{-\alpha}$ into the GSF definition given by (1) we obtain:

$$\langle |\delta x|^m \rangle = \tau^{m\alpha} \int_{-A_s}^{A_s} |\delta x_s|^m P(\delta x_s) d(\delta x_s) \propto \tau^{\zeta(m)}, \quad (3)$$

where $\tau < \tau_{max}$ and the integral now has no explicit dependence on temporal scale τ. The last proportionality in equation (3) assumes that the conditioning process does not change the scaling properties of events of size less than A. The function $\zeta(m)$ should not depend on the particular value of A selected for the conditioning. We have verified this by comparing scaling results for the range of values of the threshold $A = [8,12]\sigma(\tau)$. Equation (3) immediately relates the PDF rescaling to self-similar scaling of the GSF with $\zeta(m) = m\alpha$.

[12] The scaling properties of GSF coincide with those found for the moments of the data, computed without the absolute value operator, as long as relation (2) is valid for the PDF of differences and provided that the moments do not vanish. As we shall see, the fluctuation PDFs of *AU*, *AL* and ϵ are rather well described by a model (derived via the Fokker-Planck approach) that is symmetric. Thus, to within the statistical error of the data set, the scaling with τ given by (3) captures the behavior of the even-order moments, whereas the odd moments are small.

[13] In this approach PDFs are generated using nonoverlapping intervals of the original data. Figure 1 illustrates the difference between nonoverlapping and overlapping intervals. Let us consider a time series $x_k = x(t_k)$ with sampling time dt so that $t_k = t_0 + kdt$ and $k = 1, 2, \ldots, N$. The differences computed with nonoverlapping intervals are then given by $\delta x_j = x(t_0 + j\tau) - x[t_0 + (j-1)\tau]$. Writing time lag τ as $\tau = mdt$ we obtain $\delta x_j = x(t_0 + jmdt) - x[t_0 + (j-1)mdt]$, or in shorter notation $\delta x_j = x_{jm} - x_{(j\text{-}1)m}$, where $j = 1, 2, \ldots, [(N-1)/m] + 1$. On the other hand, for overlapping intervals we obtain $\delta x_j = x_{j+m} - x_j$ where $j = 1, 2, \ldots, N - m$. This method assures that fluctuations are not temporally correlated; an important assumption for a Fokker-Planck model we will consider later. These two methods are thus complementary as one provides a scaling exponent while the other gives an underlying probability distribution of fluctuations.

3. Results and Discussion

3.1. GSF Analysis

[14] We will first present scaling properties of the GSFs for the indices and the ϵ parameter during solar minimum and solar maximum. To illustrate the effect of conditioning, we first show, in the inset of Figure 2, a log-log plot of structure functions S_m obtained for fluctuations in the raw time series of the *AU* index at solar maximum for orders $1 \leq m \leq 6$. We see that, for orders $m > 3$ there is no clear evidence of scaling; the points do not lie on straight lines. Similar lack of scaling was also found for fluctuations in the *AL* index and the ϵ parameter. The main panel of Figure 2

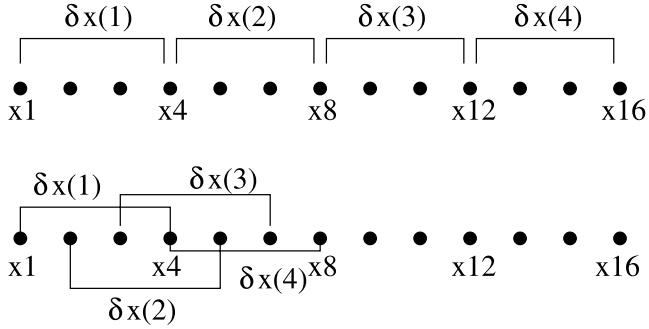

Figure 1. The use of (upper graph) nonoverlapping and (lower graph) overlapping intervals in generating difference time series.

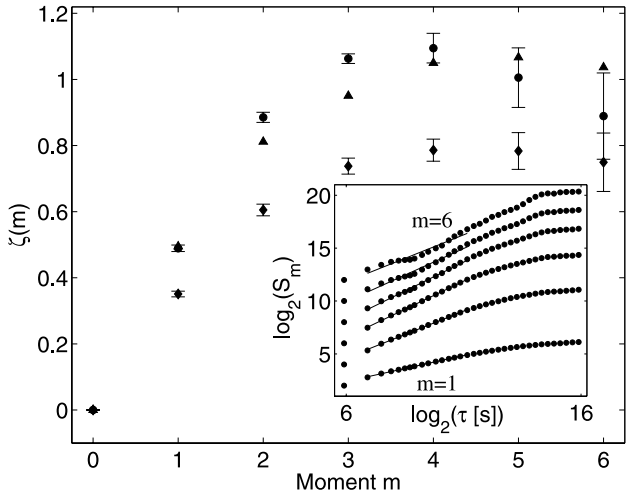

Figure 2. Exponents of unconditioned generalized structure functions as a function of order m for fluctuations in the $\epsilon(\diamond)$, $AU(\circ)$, and $AL(\triangle)$ index during solar maximum. The inset shows structure functions S_m of orders $m = 1-6$ for $\delta(AU)$.

shows exponents $\zeta(m)$ obtained by performing linear fits to logarithms of moments $log[S_m(log(\tau))]$. We see that the curves $\zeta(m)$ are not monotonic functions of m, excluding the possibility of multifractal scaling. We now condition this data set as discussed above, to check if true scaling properties are not obscured by poor statistics of extreme and very rare events. We monitored the impact of conditioning with $A = 10\sigma(\tau)$ on the original difference time series by counting the number of excluded events. In all cases no more than 1% of the given data set was eliminated.

[15] Figures 3–5 show a log-log plot of structure functions S_m for the $\delta\epsilon$, δ (AU) and δ (AL) indices at solar maximum and for order m from 1 to 6. The main indication of successfully recovered scaling after the conditioning process is the quality of the linear fit to $log[S_m(\tau)]$ versus $log(\tau)$. We clearly recover a family of straight lines with

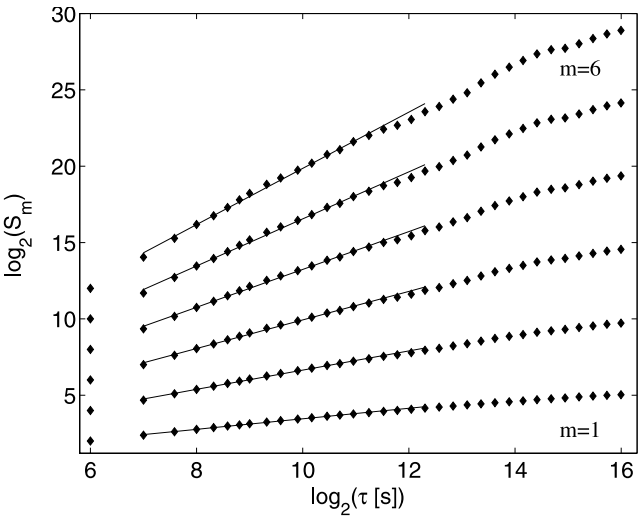

Figure 3. Structure functions S_m of orders $m = 1-6$ for fluctuations in the ϵ parameter at solar maximum.

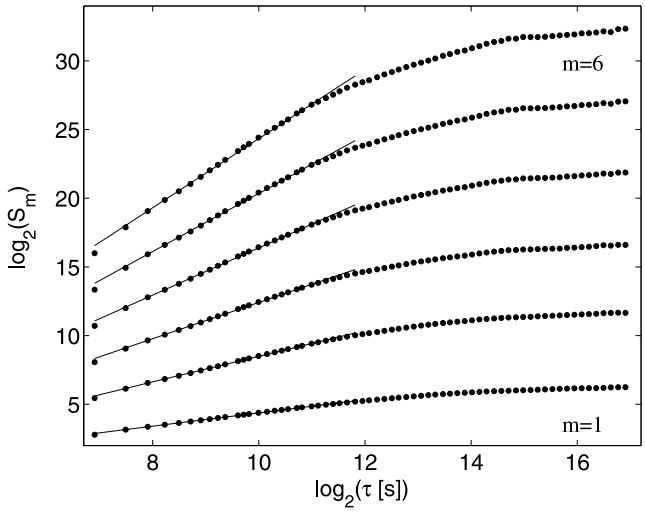

Figure 4. Same as Figure 3 for the AU index.

slopes $\zeta(m)$, up to order $m = 6$ for fluctuations in AU and AL indices and in ϵ. This scaling extends for $\sim$1.5 decades up to temporal scales of $\tau_{max} \approx 1-2$ hours in good agreement with these reported earlier [*Takalo et al.*, 1993; *Tsurutani et al.*, 1990; *Hnat et al.*, 2003a]. This corresponds to the characteristic timescale of substorms. Figure 6 shows that fluctuations in all quantities, at solar maximum, exhibit approximate self-similar scaling to within statistical errors. The error bars represent Gaussian estimates based on a least square fit of the straight line to the power law structure functions. As such they are underestimated as the processes we discuss are non-Gaussian. The size of these error bars combined with the convex shape of the function $\zeta(m)$ for the AL index also allows a weakly multifractal interpretation of the scaling. We stress, however, that the error bars in Figure 6 do not include many other uncertainties (not statistical) that are difficult to estimate. For example, the WIND spacecraft magnetometer data have absolute accuracy of about 0.1nT and the indices data have integer values

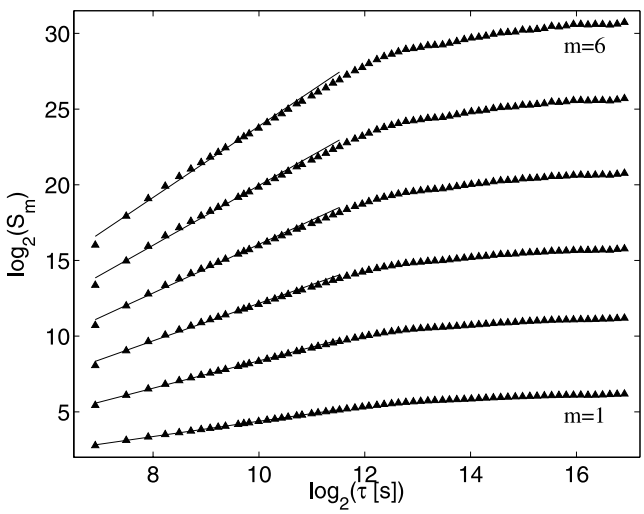

Figure 5. Same as Figure 3 for the AL index.

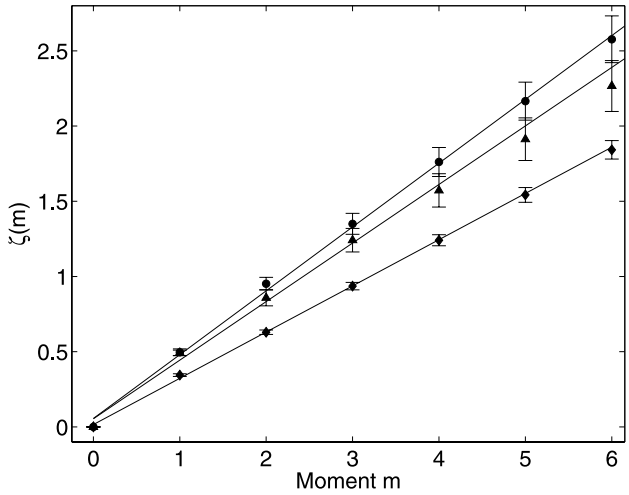

Figure 6. Exponents of conditioned generalized structure functions as a function of order m for fluctuations in the $\epsilon(\diamond)$, $AU(\circ)$, and $AL(\triangle)$ index during the solar maximum.

(also in units of nT). Such discreteness in the time series may lead to erroneous estimates of low-order moments while the finite size of the data could alter true scaling of the high-order moments. Independent of any given choice of a model for the functional form of $\zeta(m)$ we can perform a direct comparison between the $\zeta(m)$ measured for the different quantities at solar minimum and maximum. In order to develop a Fokker-Planck approach we will then make a further step and assume that a reasonable approximation is given by $\zeta(m) = m\alpha$, that is, self-similar scaling.

[16] Figures 7–9 show structure functions S_m for all quantities at solar minimum and with order m varying again from 1 to 6. We see that moments of fluctuations for the geomagnetic indices show satisfactory scaling up to temporal scales of 1–2 hours. In the case of ϵ at solar minimum there is a departure from a single set of scaling exponents $\zeta(m)$ for the smallest timescales $\tau < 12$ min. To facilitate a comparison with conditions at solar maximum and with the indices we will fit straight lines to obtain $\zeta(m)$ for $\tau =$

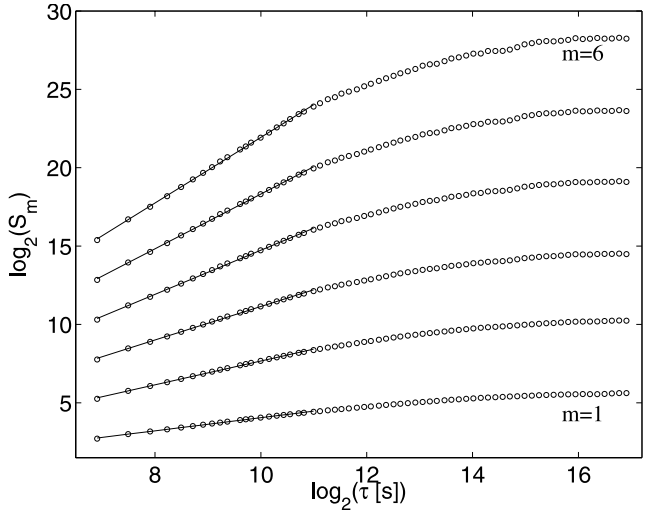

Figure 8. Same as Figure 7 for the AU index.

[12,90] min bearing in mind that this does not capture the behavior of fluctuations on the smallest timescales. This change in scaling properties for ϵ may reflect differences between solar wind evolution at solar minimum and maximum related to physical properties of slow and fast wind components [*Pagel and Balogh*, 2002]. Figure 10 is constructed identically to Figure 6 and shows scaling exponents $\zeta(m)$ for solar minimum.

[17] To make a comparison between behavior at maximum and minimum we plot, in Figure 11, exponents $\zeta(m)$ at solar minimum and maximum overplotted for AL, AU and ϵ respectively. Examining these figures we conclude that the scaling properties of the AL index fluctuations are remarkably insensitive to the change in solar activity. The values of $\zeta(m)$ and the corresponding scaling exponents are the same, to within the statistical error for solar minimum and maximum. On the other hand the scaling exponents of fluctuations in both ϵ and the AU index vary with the solar cycle. The scaling of δ (AU) is distinct from these of δ (AL) and $\delta\epsilon$ but follows the trend of $\delta\epsilon$. A possible interpretation of these

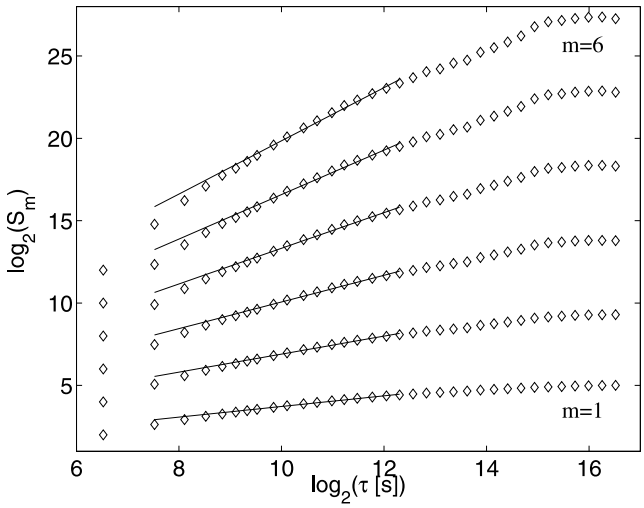

Figure 7. Structure functions S_m of orders m = 1–6 for fluctuations in the ϵ parameter at solar minimum.

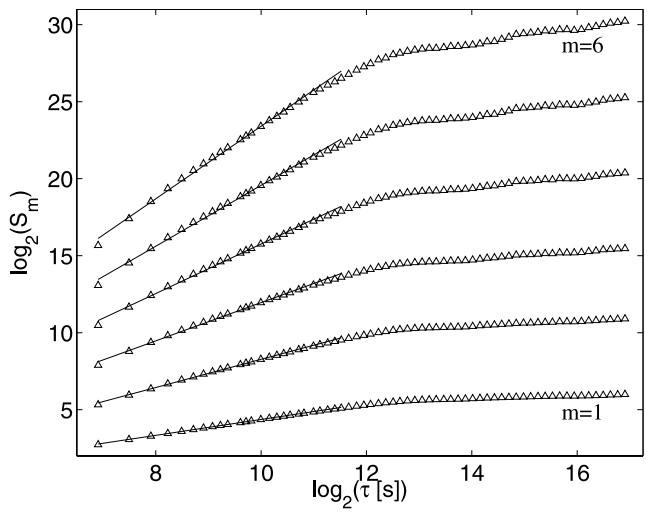

Figure 9. Same as Figure 7 for the AL index.

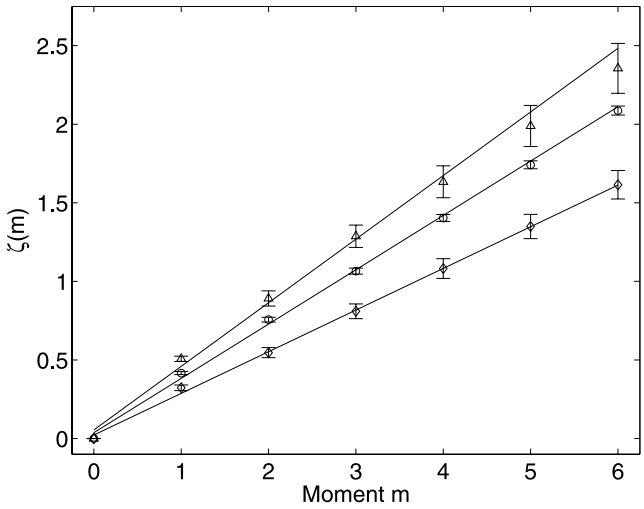

Figure 10. Same as Figure 6 for data around solar minimum.

observations is that the *AL* index fluctuations more closely reflect the internal dynamics of the magnetotail and are insulated from solar cycle related changes in the solar wind. In contrast, the *AU* index is more strongly coupled to solar cycle associated changes in the solar wind driver. This is consistent with our understanding of the global roles of these indices [e.g., *Baumjohann and Treumann*, 1996]. The fluctuations in *AU*, however, have values of scaling exponents different from that observed for the driver ϵ at solar minimum and maximum, which may suggest that (1) ϵ does not completely capture all relevant information about the driver, (2) the indices do not fully capture the magnetospheric response or (3) the difference reflects the nonlinear nature of the solar wind-magnetosphere coupling.

[18] If we compare the scaling exponents of δ (*AU*) and $\delta\epsilon$ during solar minimum and maximum we see that both quantities follow a similar trend. Closer examination of scaling exponents for fluctuations in the ϵ and the *AU* index reveals that the difference $\alpha^{AU} - \alpha^{\epsilon} \approx 0.06$ is almost identical for solar minimum and solar maximum period, to within the statistical error. This could indicate that the "conversion rate" of fluctuations in the driver to those in the *AU* index is nearly constant and independent of the strength of the driver.

[19] All scaling exponents α derived by fitting $\zeta(m) = m\alpha$ are given in the Table 2 together with the approximate maximum temporal scale τ_{max} for which self-similarity can be identified in the differenced time series. These temporal scales have been derived using R^2 goodness of fit analysis for moment with $m = 2$. We have also verified that GSF analysis of combined time series over solar minimum and maximum recovers results presented in our previous work [*Hnat et al.*, 2003a].

3.2. Probability Density Function (PDF) Rescaling

[20] We now present the results of the PDF rescaling analysis which allows us to compare directly the PDFs of the studied parameters at solar minimum and maximum. Owing to the rather poor scaling of the higher moments for the ϵ fluctuations at solar minimum we will not apply this rescaling to their PDFs. We simply state that our previous work suggested that PDFs of fluctuations in the geomagnetic indices and that of the ϵ fluctuations differed significantly when considered time interval spanned more then a solar minimum [*Hnat et al.*, 2003a].

[21] Figures 12 and 13 show rescaled PDFs of fluctuations in the *AU*, *AL* index respectively for solar minimum (empty symbols) and solar maximum (filled symbols) while Figure 14 shows these PDFs for the ϵ parameter but only at solar maximum. These PDFs correspond to the function $P_s(\delta x_s)$ in equation (2). Each plot shows overplotted $P_s(\delta x_s)$ at four temporal scales, τ = 10, 16, 26 and 42 min. These figures show data up to 10 standard deviation on any given temporal scale, consistent with the conditioning procedure described above. All rescaling exponents α used to construct these plots, are taken directly from the GSF analysis. We find that, when solar minimum and maximum data sets are taken separately, these PDFs collapse on a single curve after rescaling (2) is applied. The quality of the collapse for the PDFs was checked using the Smirnov-Kolmogorov [*Press et al.*, 1988] test and the significance of the null hypothesis (both curves drawn from the same distribution) was always found to be above the 0.975 ± 0.05 level.

[22] The rescaling confirms what we have already found by applying GSF analysis, in that a single exponent α is sufficient to give close correspondence of the curves. As we have shown in equation (3) this is consistent with approximate self-similar scaling $\zeta(m) = m\alpha$ from the GSF analysis. Once rescaled, using the values of exponents obtained separately for solar minimum and maximum, we see that the curves are distinct and the difference is most clear for the *AU* index shown in Figure 12.

[23] We also compared the functional form of these curves by applying normalization to their respective stan-

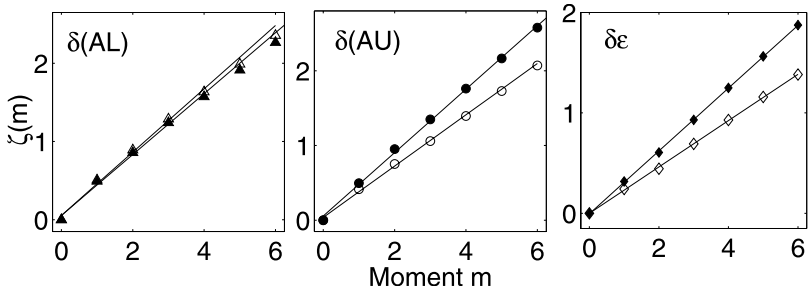

Figure 11. Comparison of functions $\zeta(m)$ during solar minimum and maximum for fluctuations in the *AL* index, *AU* index and the ϵ parameter.

Table 2. Scaling Indices Derived From GSF Analysis

Quantity	Solar Cycle	α From GSF	τ_{max}, hours
δAU	minimum	-0.35 ± 0.01	~ 1
δAU	maximum	-0.43 ± 0.01	~ 1
δAL	minimum	-0.39 ± 0.02	~ 2
δAL	maximum	-0.37 ± 0.03	~ 2
$\delta\epsilon$	minimum	-0.26 ± 0.02	~ 2
$\delta\epsilon$	maximum	-0.32 ± 0.02	~ 2

dard deviation on a given temporal scale, $\sigma_s(\tau)$. We found that the normalized PDFs for maximum and minimum are indistinguishable within the errors for *AU* and *AL*. Similar results were reported for ground based measurements of the magnetic field [*Weigel and Baker*, 2003] where authors also found that the statistics of fluctuations, when normalized to the standard deviation, is not sensitive to changing solar wind conditions.

4. The Fokker-Planck Model

[24] The Fokker-Planck (F-P) equation provides an important link between statistical properties of the system and the dynamical approach expressed by the Langevin equation [*van Kampen*, 1992]. The F-P approach can be readily applied if fluctuations are self-similar and statistically independent (uncorrelated) [*van Kampen*, 1992]. The above analysis suggests that self-similar scaling is a reasonable approximation to the data. The independent nature of increments is enforced by considering nonoverlapping intervals for differencing, as discussed in section 2.2.

[25] In the most general form the F-P equation can be written as:

$$\frac{\partial P}{\partial \tau} = \nabla_{\delta x}(A(\delta x)P + B(\delta x)\nabla_{\delta x}P), \tag{4}$$

where $P \equiv P(\delta x, \tau)$ is a PDF for the differenced quantity δx that varies with time τ and $A(\delta x)$ and $B(\delta x)$ are transport coefficients which vary with δx. It can be shown that, under the assumption of power law scaling $A(\delta x) \propto \delta x^{1-1/\alpha}$ and $B(\delta x) \propto \delta x^{2-1/\alpha}$, a class of self-similar solutions of (4) can be found that also satisfies the rescaling relation (2) [*Hnat et al.*, 2003b]. These assumptions combined with the use of rescaled variables $\delta x_s = \delta x \tau^{\alpha}$ and P_s lead to the following equation:

$$\frac{b_0}{a_0}(\delta x_s)\frac{dP_s}{d(\delta x_s)} + P_s + \frac{\alpha}{a_0}(\delta x_s)^{\frac{1}{\alpha}}P_s = C(\delta x_s)^{\frac{1}{\alpha}-1}, \tag{5}$$

where a_0, b_0, C are constants and α is the rescaling exponent derived, for example, from GSF analysis. The general solution of (5) is given by the sum of homogeneous and inhomogeneous solutions [*Chapman et al.*, 2005]:

$$P_s(\delta x_s) = \frac{a_0}{b_0}\frac{C}{|\delta x_s|^{a_0/b_0}}\exp\left(-\frac{\alpha^2}{b_0}(\delta x_s)^{1/\alpha}\right) \times \int_0^{\delta x_s} \frac{(\delta x_s')^{a_0/b_0}\exp\left(\frac{\alpha^2}{b_0}(\delta x_s')^{1/\alpha}\right)}{(\delta x_s')^{2-1/\alpha}} \cdot d(\delta x_s') + k_0 H(\delta x_s), \tag{6}$$

where k_0 is a constant and $H(\delta x_s)$ is the homogeneous solution:

$$H(\delta x_s) = \frac{1}{|\delta x_s|^{a_0/b_0}}\exp\left(-\frac{\alpha^2}{b_0}(|\delta x_s|)^{1/\alpha}\right). \tag{7}$$

The simple model described above assumes that self-similar scaling persists for all δx. This assumption is expected to hold for a physical system for a large but finite range of δx. In particular, it will break down as $\delta x_s \rightarrow 0$ giving a singularity in the solution P_s as $\delta x_s \rightarrow 0$. This singularity is integrable for $0 \leq a_0/b_0 \leq 1$ and outside of this range can be considered as an asymptotic solution.

[26] We have found that fluctuations in the geomagnetic indices in solar minimum and maximum and these in ϵ at solar maximum exhibit self-similar statistics to a reasonable approximation. We will now show that the functional form of the PDF obtained from the F-P model (6) is a good approximation for the observed rescaled distribution $P_s(\delta x_s)$ of fluctuations shown in Figures 12–14. On Figures 12–14 we have overplotted solution (6), shown by thick dashed line, with α taken to be that obtained from the GSF analysis. Table 3 gives values of all parameters assumed for each of the plotted solutions. Although the F-P solutions obtained here are symmetric, they provide a good fit to the fluctuation PDFs, to within errors, as we can see in Figures 12–14. However, the PDF of fluctuations in geomagnetic indices do posses a weak asymmetry [*Hnat et al.*, 2003a] that leads to small departures of the predicted curves from the observed ones.

[27] We note an obvious departure of our predicted curves from the measured PDF for the smallest fluctuations, in all considered cases. This is due to the functional form of (7) where $H(\delta x_s) \rightarrow \infty$ when $\delta x_s \rightarrow 0$ arising from the assumption that the self-similar scaling extends to arbitrary small fluctuations. To model this part of the curve, we

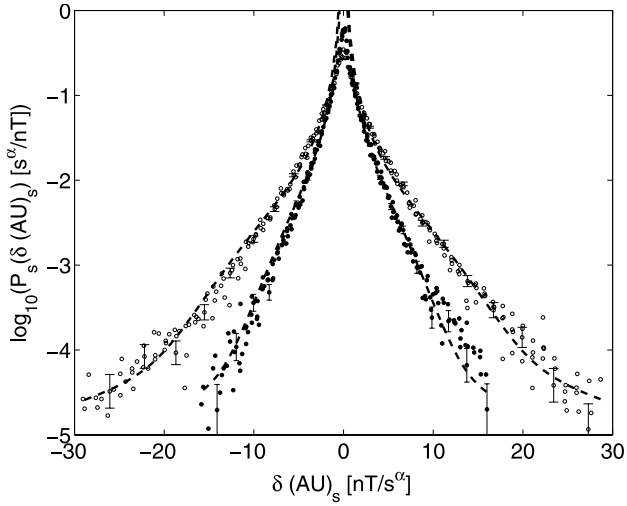

Figure 12. Rescaled PDFs of the $\delta(AU)$ during solar minimum (open symbols) and maximum (filled symbols). Symbols correspond to temporal scales τ = 10, 16, 26, and 42 min. The dashed line represents a solution of the Fokker-Planck model (equation (6)) with parameters given in Table 3. See color version of this figure at back of this issue.

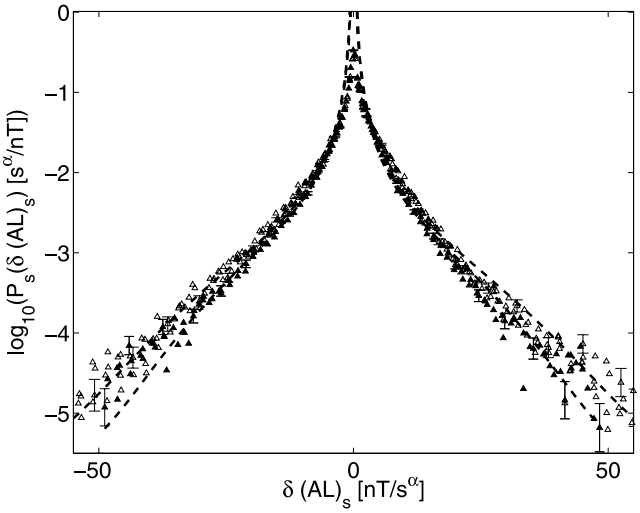

Figure 13. Same as Figure 12 for the *AL* index fluctuations. See color version of this figure at back of this issue.

would need to include the scaling, or lack of thereof, introduced by the uncertainty in the measurements. We would expect such processes to be dominant for the smallest fluctuations. For example, if we assume that the smallest fluctuations are dominated by Normally distributed noise, then a diffusion model with a constant diffusion coefficient D_0 could, in principle, be used to tame this singular behavior. This stochastic approach can be extended to obtain the Langevin equation for the dynamics of the fluctuations [*Hnat et al.*, 2003b]. The Langevin equation can be written in the most general form as:

$$\frac{d(\delta x)}{dt} = \beta(\delta x) + \gamma(\delta x)\xi(t), \tag{8}$$

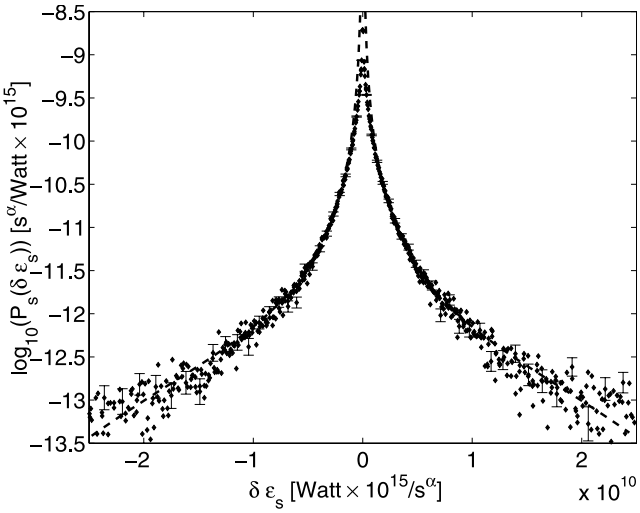

Figure 14. Same as Figure 12 for the ϵ parameter fluctuations at solar maximum. See color version of this figure at back of this issue.

Table 3. Values of Parameters Used for F-P Model Solutions Plotted in Figures 12–14

Quantity	Solar Cycle	b_0	a_0/b_0	k_0	C
δAU	minimum	190	1.875	0.28	6×10^{-7}
δAU	maximum	16	1.875	0.20	1×10^{-5}
δAL	minimum	1200	1.85	0.36	5×10^{-6}
δAL	maximum	1200	1.85	0.32	7.5×10^{-6}
$\delta\epsilon$	maximum	2×10^{30}	2.15	2.5×10^{9}	1×10^{-34}

where the random variable $\xi(t)$ is assumed to be δ-correlated. Equation 8 can be transform into purely additive noise form:

$$\frac{dz}{dt} = \frac{\beta(z)}{\gamma(z)} + \xi(t), \tag{9}$$

where $z = \int_0^{\delta x} 1/\gamma(\delta x')\, d(\delta x')$. It has been shown [*Hnat et al.*, 2003b] that one can obtain a functional form of coefficients $\beta(\delta x)$ and $\gamma(\delta x)$ in terms of a_0, b_0 (from equation 5) and the scaling exponent α. Such an equation provides a dynamical model for time series with the required statistical properties.

5. Summary

[28] The response of the Earth's magnetosphere to the solar cycle and, by implication, a changing character of solar wind activity, illuminates the interplay between intrinsic magnetospheric dynamics and solar wind-magnetosphere coupling. Statistical studies provide a simple and yet unifying way to quantify this behavior in the context of models for intermittency. In this paper we considered scaling properties of the solar wind driver, quantified by the ϵ parameter, and geomagnetic indices during solar minimum and maximum. We emphasize that the conditioning procedure applied to a differenced time series eliminates the most extreme events from the data. In the case of ϵ this procedure excludes some features of the large coherent structures in the solar wind, such as shocks or mirror mode structures. In this sense the conclusions of our investigation apply predominantly to the interaction between ambient solar wind and the magnetosphere. Also, consistent with previous studies we find scaling in the geomagnetic indices on timescales shorter than 1–2 hours, that is shorter than the characteristic substorm timescale. This choice of temporal scales then naturally excludes substorm features from our comparative study. We find that:

[29] 1. Fluctuations in the geomagnetic indices show approximate statistical self-similarity for a range of temporal scales. Fluctuations in the ϵ at solar minimum show departure from scaling for $\tau < \sim 10$ min. The self-similar scaling emerges as a reasonable approximation for fluctuations $\delta\epsilon$ at solar maximum. Fluctuations in the geomagnetic indices exhibit self-similar scaling on temporal scales between $\sim$2 min to $\sim$1–2 hours. The fluctuations in ϵ scales from $\sim$2 min to $\sim$1.5 hours, but only at solar maximum.

[30] 2. Fluctuations in the *AL* index exhibit scaling properties insensitive to the phase of the solar cycle.

[31] 3. The scaling exponent of $\delta(AU)$ changes with the solar cycle and the trend follows that of the ϵ parameter.

[32] 4. The value of the scaling exponents of indices and that of the ϵ parameter differ from each other at both solar minimum and maximum. This difference between scaling exponents of $\delta(AU)$ and the driver $\delta\epsilon$ is approximately the same at solar minimum and maximum.

[33] 5. A Fokker-Planck approach can be used to model the fluctuation PDF for the geomagnetic indices in both phases of the solar cycle and the ϵ at solar maximum to a good approximation.

[34] The approximate statistical self-similarity found for the indices for solar minimum and maximum and the ϵ at solar maximum is consistent with complex multiscale processes such as turbulence or self-organized criticality (SOC). The distinct values found for scaling exponents may reflect physical differences in the solar wind and the magnetosphere but may also be due to the very different way in which these quantities are derived. The fluctuations in the AU index depend on the solar cycle but the scaling exponent is distinct from that of ϵ fluctuations. Interestingly, the difference between scaling exponents of $\delta(AU)$ and the driver $\delta\epsilon$ appears to be approximately constant. These observations, when combined together, suggest that the process involved in generating fluctuations in the AU index is coupled to the solar wind driver, as seen in the solar cycle dependence. In contrast to the AU index fluctuations, these in the AL index are nearly insensitive to the change in solar cycle implying that the AL index is a measure of activity intrinsic to the magnetosphere. This is consistent with the AU index more closely monitoring activity on the dayside and AL reflecting activity in the magnetotail.

[35] The self-similar scaling of fluctuations allows us to model their statistics using a Fokker-Planck approach. We obtained analytically a functional form of the fluctuation PDF which approximates the measured PDF rather well. We stress that such an approach links the statistical features discussed here to dynamical modeling of the time series via stochastic Langevin equations.

[36] **Acknowledgments.** B. Hnat acknowledges support from the PPARC, S. C. Chapman from the Radcliffe Institute, and G. Rowlands from the Leverhulme Trust. We thank R. P. Lepping and K. Ogilvie for provision of data from the NASA WIND spacecraft, the ACE SWEPAM instrument team, and the ACE Science Center for providing the ACE data and the WDC for the geomagnetic indices data.

[37] Lou-Chuang Lee thanks Wendell Horton and A. J. Klimas for their assistance in evaluating this paper.

References

Angelopoulos, V., W. Baumjohann, C. F. Kennel, F. V. Coroniti, M. G. Kivelson, R. Pellat, R. J. Walker, H. Lühr, and G. Paschmann (1992), Bursty bulk flows in the inner central plasma sheet, *J. Geophys. Res.*, *97*(A4), 4027–4039.

Angelopoulos, V., T. Mukai, and S. Kokubun (1999), Evidence for intermittency in Earth's plasma sheet and implications for self-organized criticality, *Phys. Plasmas*, *6*(11), 4161–4168.

Baumjohann, W., and R. A. Treumann (1996), *Basic Space Plasma Physics*, pp. 89–100, Imperial College Press, London.

Chang, T. (1992), Low-dimensional behavior and symmetry breaking of stochastic systems near criticality: Can these effects be observed in space and in the laboratory?, *IEEE Trans. Plasma Sci.*, *20*, 691.

Chapman, S. C., and N. W. Watkins (2001), Avalanching and self organised criticality: a paradigm for magnetospheric dynamics?, *Space Sci. Rev.*, *95*, 293–307.

Chapman, S. C., B. Hnat, G. Rowlands, and N. W. Watkins (2005), Scaling collapse and structure functions: Identifying self-affinity in finite length time series, *Nonlinear Processes Geophys.*, *12*, 767–774.

Consolini, G., and P. De Michelis (1998), Non-Gaussian distribution function of AE-index fluctuations: Evidence for time intermittency, *Geophys. Res. Lett.*, *25*, 4087–4090.

Consolini, G., M. F. Marcucci, and M. Candidi (1996), Multifractal structure of auroral electrojet index data, *Phys. Rev. Lett.*, *76*, 4082–4085.

Freeman, M. P., N. W. Watkins, and D. J. Riley (2000), Evidence for a solar wind origin of the power law burst lifetime distribution of the AE indices, *Geophys. Res. Lett.*, *27*, 1087–1090.

Frisch, U. (1995), *Turbulence: The Legacy of A. N. Kolmogorov*, 89 pp., Cambridge Univ. Press, New York.

Hnat, B., S. C. Chapman, G. Rowlands, N. W. Watkins, and M. P. Freeman (2003a), Scaling in long term data sets of geomagnetic indices and solar wind e as seen by WIND spacecraft, *Geophys. Res. Lett.*, *30*(22), 2174, doi:10.1029/2003GL018209.

Hnat, B., S. C. Chapman, and G. Rowlands (2003b), Intermittency, scaling, and the Fokker-Planck approach to fluctuations of the solar wind bulk plasma parameters as seen by the WIND spacecraft, *Phys. Rev. E*, *67*, 056404.

Horbury, T. S., and A. Balogh (1997), Structure function measurements of the intermittent MHD turbulent cascade, *Nonlinear Proc. Geophys.*, *4*, 185–199.

Horton, W., J. P. Smith, R. Weigel, C. Crabtree, I. Doxas, and B. Goode (1999), The solar-wind driven magnetosphere-ionosphere as a complex dynamical system, *Phys. Plasmas*, *6*(11), 4178–4184.

Klimas, A. J., D. Vassiliadis, D. N. Baker, and D. A. Roberts (1996), The organized nonlinear dynamics of the magnetosphere, *J. Geophys. Res.*, *101*, 13,089–13,113.

Klimas, A., V. Uritsky, and D. Baker (2004a), Scale-free avalanching and a loading-unloading cycle in a driven current-sheet model, paper presented at International Conference on Substorms-7, Finnish Meteorol. Inst., Helsinki.

Klimas, A. J., V. M. Uritsky, D. Vassiliadis, and D. N. Baker (2004b), Reconnection and scale-free avalanching in a driven current-sheet model, *J. Geophys. Res.*, *109*, A02218, doi:10.1029/2003JA010036.

Kovács, P., V. Carbone, and Z. Vörös (2001), Wavelet-based filtering of intermittent events from geomagnetic time series, *Planet. Space Sci.*, *49*, 1219–1231.

Kozelov, B. V., and T. V. Kozelova (2003), Cellular automata model of magnetospheric-ionospheric coupling, *Annal. Geophys.*, *21*(9), 1931–1938.

Kozelov, B. V., V. M. Uritsky, and A. J. Klimas (2004), Power law probability distributions of multiscale auroral dynamics from ground-based TV observations, *Geophys. Res. Lett.*, *31*, L20804, doi:10.1029/2004GL020962.

Lewis, Z. V. (1991), On the apparent randomness of substorm onset, *Geophys. Res. Lett.*, *18*(8), 1627–1630.

Lui, A. T. Y., S. C. Chapman, K. Liou, P. T. Newell, C. I. Meng, M. Brittnacher, and G. K. Parks (2000), Is the dynamic magnetosphere an avalanching system?, *Geophys. Res. Lett.*, *27*(7), 911–914.

Pagel, C., and A. Balogh (2002), Intermittency in the solar wind: A comparison between solar minimum and maximum using Ulysses data, *J. Geophys. Res.*, *107*(A8), 1178, doi:10.1029/2002JA009331.

Perreault, P., and S.-I. Akasofu (1978), A study of geomagnetic storms, *Geophys. J. R. Astron. Soc.*, *54*, 547–573.

Press, W. H., B. P. Flannery, S. A. Teukolsky, and W. T. Vetterling (1988), *Numerical Recipes in C*, 490 pp., Cambridge Univ. Press, New York.

Sitnov, M. I., A. S. Sharma, K. Papadopoulos, D. Vassiliadis, J. A. Valdivia, A. J. Klimas, and D. N. Baker (2000), Phase transition-like behavior of the magnetosphere during substorms, *J. Geophys. Res.*, *105*, 12,955–12,974.

Sornette, D. (2000), *Critical Phenomena in Natural Sciences; Chaos, Fractals, Selforganization and Disorder: Concepts and Tools*, Springer, New York.

Stepanova, M. V., E. E. Antonova, and O. Troshichev (2003), Intermittency of magnetospheric dynamics through non-Gaussian distribution function of PC-index fluctuations, *Geophys. Res. Lett.*, *30*(3), 1127, doi:10.1029/2002GL016070.

Takalo, J., J. Timonen, and H. Koskinen (1993), Correlation dimension and affinity of AE data and bicolored noise, *Geophys. Res. Lett.*, *20*, 1527–1530.

Takalo, J., K. Mursula, and J. Timonen (2000), Role of the driver in the dynamics of a coupled-map model of the magnetotail: Does the magnetosphere act as a low-pass filter?, *J. Geophys. Res.*, *105*, 27,665–27,672.

Tsurutani, B. T., M. Sugiura, T. Iyemori, B. E. Goldstein, W. D. Gonzalez, S. I. Akasofu, and E. J. Smith (1990), The nonlinear response of AE to the IMF B_s driver: A spectral break at 5 hours, *Geophys. Res. Lett.*, *17*, 279–282.

Ukhorskiy, A. Y., M. I. Sitnov, A. S. Sharma, and K. Papadopoulos (2003), Combining global and multi-scale features in a description of

the solar wind-magnetosphere coupling, *Annal. Geophys.*, *21*(9), 1913–1929.

Uritsky, V. M., and M. I. Pudovkin (1998), Low frequency 1/f-like fluctuations of the AE-index as a possible manifestation of self-organized criticality in the magnetosphere, *Annal. Geophys.*, *16*(12), 1580–1588.

Uritsky, V. M., A. J. Klimas, and D. Vassiliadis (2001), Comparative study of dynamical critical scaling in the auroral electrojet index versus solar wind fluctuations, *Geophys. Res. Lett.*, *28*, 3809–3812.

Uritsky, V. M., A. J. Klimas, and D. Vassiliadis (2002a), Multiscale dynamics and robust critical scaling in a continuum current sheet model, *Phys. Rev. E*, *65*(4), 046113.

Uritsky, V. M., A. J. Klimas, D. Vassiliadis, D. Chua, and G. Parks (2002b), Scale-free statistics of spatiotemporal auroral emissions as depicted by POLAR UVI images: Dynamic magnetosphere is an avalanching system, *J. Geophys. Res.*, *107*(A12), 1426, doi:10.1029/2001JA000281.

Uritsky, V. M., A. J. Klimas, and D. Vassiliadis (2003), Evaluation of spreading critical exponents from the spatiotemporal evolution of emission regions in the nighttime aurora, *Geophys. Res. Lett.*, *30*(15), 1813, doi:10.1029/2002GL016556.

van Kampen, N. G. (1992), *Stochastic Processes in Physics and Chemistry*, North-Holland, New York.

Vassiliadis, D., A. J. Klimas, J. A. Valdivia, and D. N. Baker (2000), The nonlinear dynamics of space weather, *Adv. Space. Res.*, *26*, 197–207.

Vassiliadis, D., R. S. Weigel, A. J. Klimas, S. G. Kanekal, and R. A. Mewaldt (2003), Modes of energy transfer from the solar wind to the inner magnetosphere, *Phys. Plasmas*, *10*(2), 463–473.

Vörös, Z., P. Kovács, A. Juhász, A. Körmendi, and A. W. Green (1998), Scaling laws from geomagnetic time series, *J. Geophys. Res.*, *103*, 2621–2624.

Vörös, Z., D. Jankovièová, and P. Kovács (2002), Scaling and singularity characteristics of solar wind and magnetospheric fluctuations, *Nonlinear Proc. Geophys.*, *9*(2), 149–162.

Weigel, R. S., and D. N. Baker (2003), Probability distribution invariance of 1-minute auroral-zone geomagnetic field fluctuations, *Geophys. Res. Lett.*, *30*(23), 2193, doi:10.1029/2003GL018470.

Weigel, R. S., A. J. Klimas, and D. Vassiliadis (2003), Solar wind coupling to and predictability of ground magnetic fields and their time derivatives, *J. Geophys. Res.*, *108*(A7), 1298, doi:10.1029/2002JA009627.

S. C. Chapman, B. Hnat, and G. Rowlands, Space and Astrophysics Group, University of Warwick, Coventry CV4 7AL, UK. (hnat@astro.warwick.ac.uk)

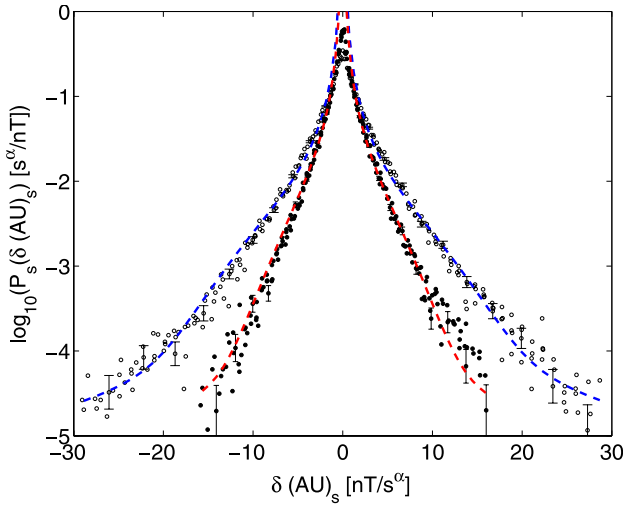

Figure 12. Rescaled PDFs of the $\delta(AU)$ during solar minimum (open symbols) and maximum (filled symbols). Symbols correspond to temporal scales τ = 10, 16, 26, and 42 min. The dashed line represents a solution of the Fokker-Planck model (equation (6)) with parameters given in Table 3.

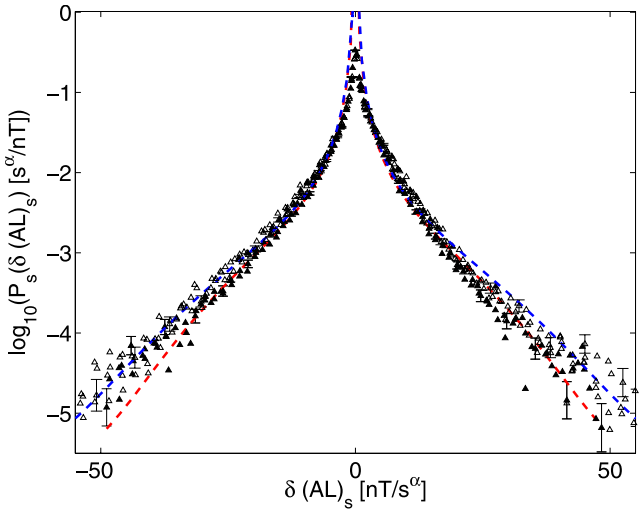

Figure 13. Same as Figure 12 for the *AL* index fluctuations.

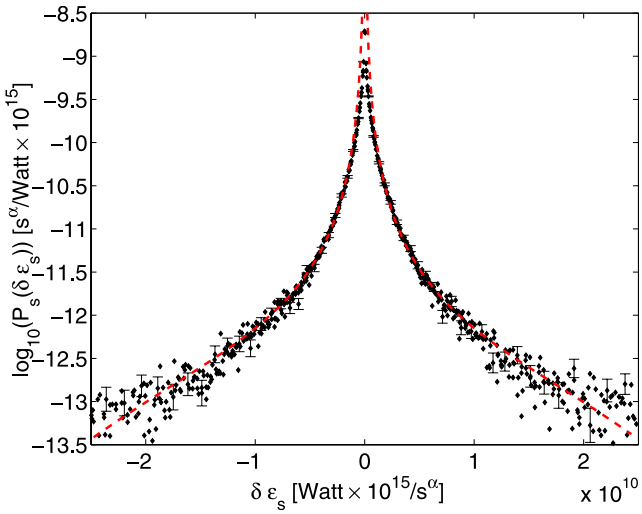

Figure 14. Same as Figure 12 for the ϵ parameter fluctuations at solar maximum.